UDC 544.72 : 544.18

M.T. Kartel, V.S. Kuts, A.G. Grebenyuk, Yu.A. Tarasenko

COMPARATIVE QUANTUM CHEMICAL EXAMINATION OF LITHIATION/DELITHIATION PROCESSES IN Si_n NANOCLUSTERS AND C_mSi_n NANOCOMPOSITES

Chuiko Institute of Surface Chemistry of National Academy of Sciences of Ukraine
17 General Naumov Str., Kyiv, 03164, Ukraine, E-mail: kutsvs08@rambler.ru

A comparative quantum chemical (PM3 method) examination has been carried out of lithiation/delithiation processes in Si_n nanoclusters and C_mSi_n nanocomposites. These processes in the nanocomposites (25 and ~30 % C, respectively) have been shown to effect slightly on the volumes and structures of initial (C_mSi_n), lithiated ($Li_{k=0-52}C_mSi_n$), and delithiated ($Li_{k=52-0}C_mSi_n$) silicon-carbon matrices Si/C. Electrodes from such materials should not undergo destructive effect of periodic deformations in charge/discharge cycles. On the contrary, at lesser carbon concentrations (C_6Si_{13} nanocomposite, ~16 % C) lithiation results in the 1.8 times hopping expansion of $V(C_6Si_{13})$, and delithiation – in the change in structure of initial silicon-carbon matrix Si/C. For Si/C electrodes with greater (more than 37 %) carbon concentration ($C_{m>18}Si_n$ composites), lithiation results in a monotonous increase in the volume (1.3 times for $C_{18}Si_{13}$ and 1.5 times for $C_{26}Si_{13}$) whereas delithiatin leads to a considerable change in the initial structure of silicon-carbon matrix.

Keywords: *silicon nanoclusters, silicon-carbon nanocomposites, lithiation/delithiation, specific volume, semiempirical quantum chemical treatment*

INTRODUCTION

Recently, electrode materials based on silicon-lithium electrochemical alloys have been paid a great attention. Indeed, theoretically calculated specific capacity of such alloys, in particular that of $Li_{15}Si_4$, reaches 3579 mA·h/g, what is close enough to that of lithium metal (4235 mA·h/g) [1, 2]. Nevertheless, lithiation/delithiation of silicon nanoclusters results in the 2–3 times increase in their volume causing local mechanical strains in the electrode material and so in shunt contact loss and in a decrease in quantitative and qualitative cycling characteristics [2–4]. In [5] the lithiation/delithiation process was simulated taking Si_{12} nanocluster as an example as well as Li_kSi_{12} nanoalloys. The lithiation process (k → 0–48) was shown to result in fragmenting the Si_n nanocluster whereas delithiation (k → 48–0) changed the spatial and electronic structure of initial cluster.

Covering silicon micro- or nanoparticles with carbon is shown in [6–14] to result in an increase in the reversible capacity and the number of charge-discharge cycles of silicon-carbon (Si/C) electrodes as well as of the Coulomb component of the first cycle. Si/C composites are produced by various methods: powdering silicon mixed with graphite in a ball mill, deposition of carbon atoms from gas phase (or plasma), pyrolysis of a silicon mixture with carbon-containing precursors [15–20]. Such preparation modes for Si/C-composites provide deposition or adsorption of both individual carbon atoms and their associates (C_n, where $n = 2, 3$ and so on) onto the surfaces of silicon clusters with probable formation of more heavy fragments of both amorphous and ordered carbon nanostructures, in particular those characterized by sp^2-hybridization of atomic orbitals (fullerenes, graphenes, nanotubes).

This paper describes the results of quantum chemical studies on the electronic structures of Si/C-nanocomposites C_mSi_n with various atomic ratios.

MODELS AND METHODS

The penetration effect of lithium atoms under lithiation into C_mSi_n nanocomposites on the spatial and electronic structures of nanoalloys $Li_kC_mSi_n$ formed was examined by semiempirical method PM3 by means of GAMESS program package [21]. The spatial structures of clusters Si_n was borrowed from [5]. The starting coordinates of

carbon atoms in the C_mSi_n nanocomposites and those of lithium atoms in the Li_kSi_n and $Li_kC_mSi_n$ nanoalloys were determined by method of molecular mechanics by means of HyperChem7 program package, the electrostatic and non-specific interactions between the host cluster (Si_n) and addition atoms (Li, C) being described adequately. So, found initial coordinates of the systems under study were used for calculations of the electronic structures of Si_n nanoclusters, C_mSi_n nano-composites as well as of Li_kSi_n and $Li_kC_mSi_n$ nanoalloys. When calculating the volume values (*V*) of the Si_n subclusters in the nanocomposites and nanoalloys mentioned, the MOPAC 2012 14.083W [22] program was used. For all the nanosystems studied, spatial structures, atomic net charge densities (ρ), the energy values for the frontier molecular orbitals (highest occupied E_{HOMO} and lowest unoccupied E_{LUMO}), and the local densities of the states over atoms (Si, C, and Li) were found.

RESULTS AND DISCUSSION

Let us consider the structure of C_mSi_n nanocomposites in detail, the nanosystems with the fixed number of silicon atoms C_mSi_{13} (Figs. 1 and 2) being examples. It should be noted that the accepted spatial structure of the nanocluster is consistent with those of the most stable isomers of nanocluster Si_{13} found by *ab initio* methods (DFT, UHF) [23–25].
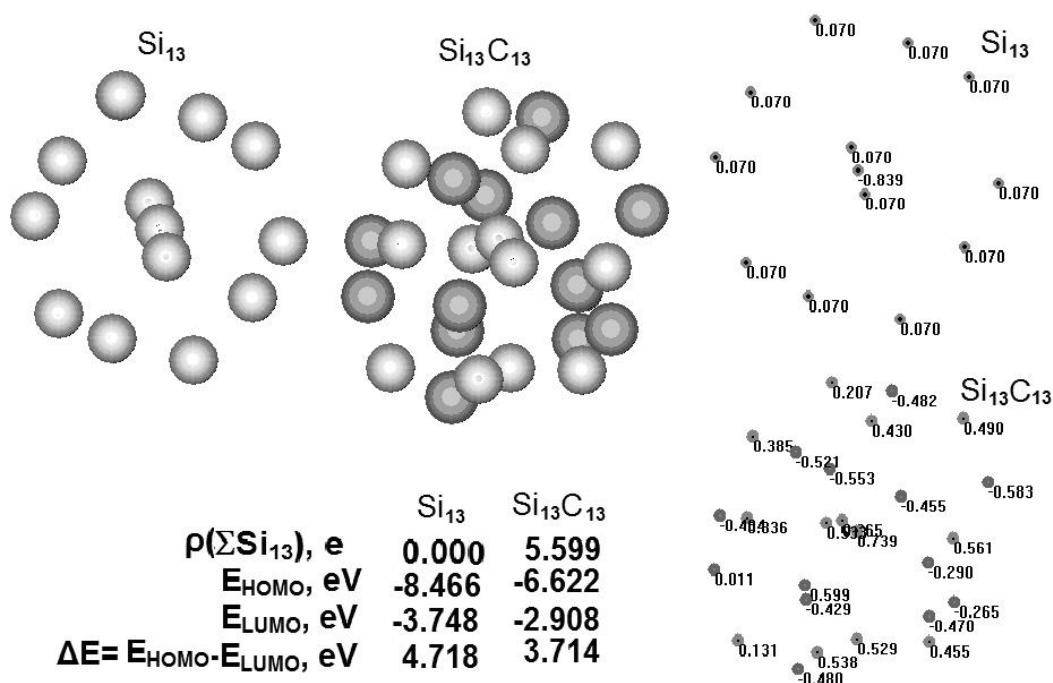

	Si_{13}	$Si_{13}C_{13}$
$\rho(\Sigma Si_{13})$, e	0.000	5.599
E_{HOMO}, eV	-8.466	-6.622
E_{LUMO}, eV	-3.748	-2.908
$\Delta E = E_{HOMO}-E_{LUMO}$, eV	4.718	3.714

Fig. 1. Spatial structures, electronic and energy characteristics of Si_{13} nanocluster and of $C_{13}Si_{13}$ nanocomposite

The results of calculations of the structure, charge distribution, energies of the frontier molecular orbitals in C_{13} nanocluster and in $C_{13}Si_{13}$ nanocomposite (Fig. 1) testify as follows:

1. Large positive charges ($\rho Si_i > 0$) are located on the silicon atoms of Si_{13} subcluster in the $C_{13}Si_{13}$ nanocomposite (as compared to those in the initial Si_{13} nanocluster) whereas carbon atoms in the C_{13} subcluster of this nanocomposite are negatively charged ($\rho C_i < 0$).

2. In the $C_{13}Si_{13}$ nanocomposite a considerable redistribution takes place of electron density between the Si_{13} and C_{13} subclusters ($\rho \Sigma Si_{13} > 0$).

3. The electron donor capability of $C_{13}Si_{13}$ nano-composite increases $\{E_{HUMO}(C_{13}Si_{13}) > E_{HUMO}(Si_{13})\}$ and the electron acceptor one decreases $\{E_{LUMO}(C_{13}Si_{13}) > E_{LUMO}(Si_{13})\}$; in addition, a decrease is also observed in the width of forbidden zone $\Delta E(C_{13}Si_{13}) = E_{LUMO} - E_{HUMO}$ (as compared to that of Si_{13} nanocluster) what testifies potentially greater electron mobility in the $C_{13}Si_{13}$ nanocomposite.

It is seen also in Fig. 1 that the marginal atoms of Si_{13} nanocluster bear negligible positive charges (0.070 e) whereas those in the $C_{13}Si_{13}$ nano-composite reach considerable values (within

0.131–0.538 e). Carbon atoms in the $C_{13}Si_{13}$ nanocomposite bear, mostly, negative charges with values within –0.265 to −0.583 e. That is why the surface electrostatic potential in the nanocomposite should include both electrophilic (near silicon atoms) and nucleophilic (near carbon atoms) areas. Thus, when added to nanocomposites C_mSi_n, lithium atoms should be stationed near electrophilic areas, i.e. near silicon atoms. The results obtained allow us to believe that the electrochemical processes of lithiation/delithiation in Si_n nanoclusters and in C_mSi_n nanocomposites differ substantially.

In C_mSi_{13} nanocomposites at the values $m/13 \leq 1$, dimensions and structures of Si_{13} subclusters do not change practically (the volume ratio $V(Si_{13}):V(C_{m \leq 13}Si_{13})$ increases only for 4.5 %); at the same time all carbon atoms in the nanocomposite are stationed at the periphery of Si_{13} subcluster (Fig. 2).

In C_mSi_{13} nanocomposites at $m=20, 26, 39$, and 45 a considerable destruction is observed of the initial structures Si_{13} as well as an increase in the volume ratio $V(Si_{13}) / V(C_mSi_{13})$ respectively for 12.8 to 33.2 %. The structures of $C_{m>13}Si_{13}$ nanocomposites most probably resemble a solution of silicon atoms in a carbon matrix, what agrees with data [11]. The results of calculations of atomic coordinates of carbon atoms in C_m subclusters testify that at $m/n \leq 1$ interatomic distances are more than 2.6 Å (there are no chemical bonds C–C). In the composites at $m/n>1$, carbon associates C_2, C_3, C_4 and so on are observed, interatomic distances being within 1.2–1.3 Å, what testifies formation of covalent bonds.

C_mSi_n	Si_{13}	C_6Si_{13}	$C_{10}Si_{13}$	$C_{13}Si_{13}$
m/n	0	0.462	0.769	1
$V(C_mSi_{13})$, Å³ / $V(Si_{13/m})$, Å³	$\frac{400}{400}=1$	$\frac{445}{442}=1.007$	$\frac{466}{463}=1.006$	$\frac{511}{489}=1.045$

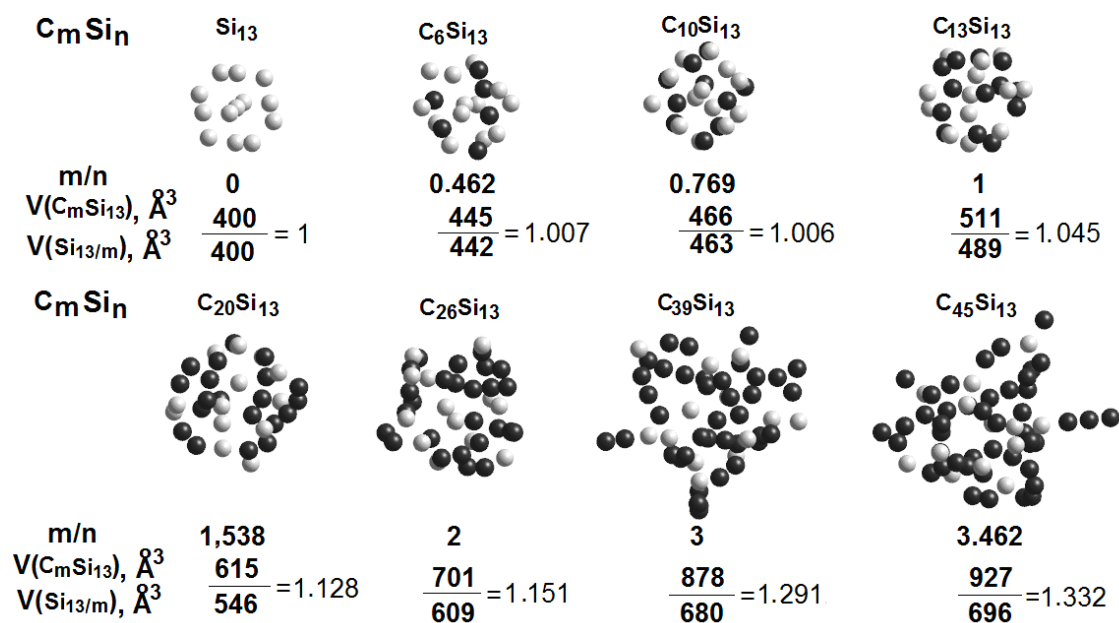| C_mSi_n	$C_{20}Si_{13}$	$C_{26}Si_{13}$	$C_{39}Si_{13}$	$C_{45}Si_{13}$
m/n	1,538	2	3	3.462
$V(C_mSi_{13})$, Å³ / $V(Si_{13/m})$, Å³	$\frac{615}{546}=1.128$	$\frac{701}{609}=1.151$	$\frac{878}{680}=1.291$	$\frac{927}{696}=1.332$

Fig. 2. Structures of C_mSi_n nanocomposites

The results obtained give reasons to insist that in the C_mSi_n nanocomposites Si_n nanoclusters may by covered with carbon coating consiting of both individual carbon atoms and associates $C_{m<4}$. Besides, as it is seen in Fig. 2, in the nanocomposites with enlarged carbon content ($C_{39}Si_{13}$ and $C_{45}Si_{13}$) $C_{m1<m}Si_{n1<n}$ subcomposites are formed as well as silicon Si_{n2} and carbon C_{m2} subclusters, lithium atoms being embedded into interparticle space.

It is also follows from the calculations that an increase in the number of carbon atoms near cluster Si_n surface results in a positive shift of the energies of frontier molecular orbitals E_{HOMO} and E_{LUMO} (Fig. 3 a); at the same time a considerable decrease in the width of forbidden zone ΔE (almost for 1 eV) is observed for composite nanosystems where the values m and n are close. The latter testifies the greater electron exchange mobility between Si_n and C_m subsystems in the C_mSi_n nanocomposites. It should be also noted that an increase in the number of carbon atoms near nanocluster Si_n surface causes an increase in the total positive charge on silicon atoms (Fig. 3 b) due to electron density transfer from subcluster Si_n to C_m one where relative total negative charge is

accumulated. Besides, one can claim that the electrophility of C_mSi_n nanocomposites is higher essentially than that of Si_n nanoclusters. Obviuosly, this fact facilitates penetration of lithium atoms into Si/C nanocomposites.
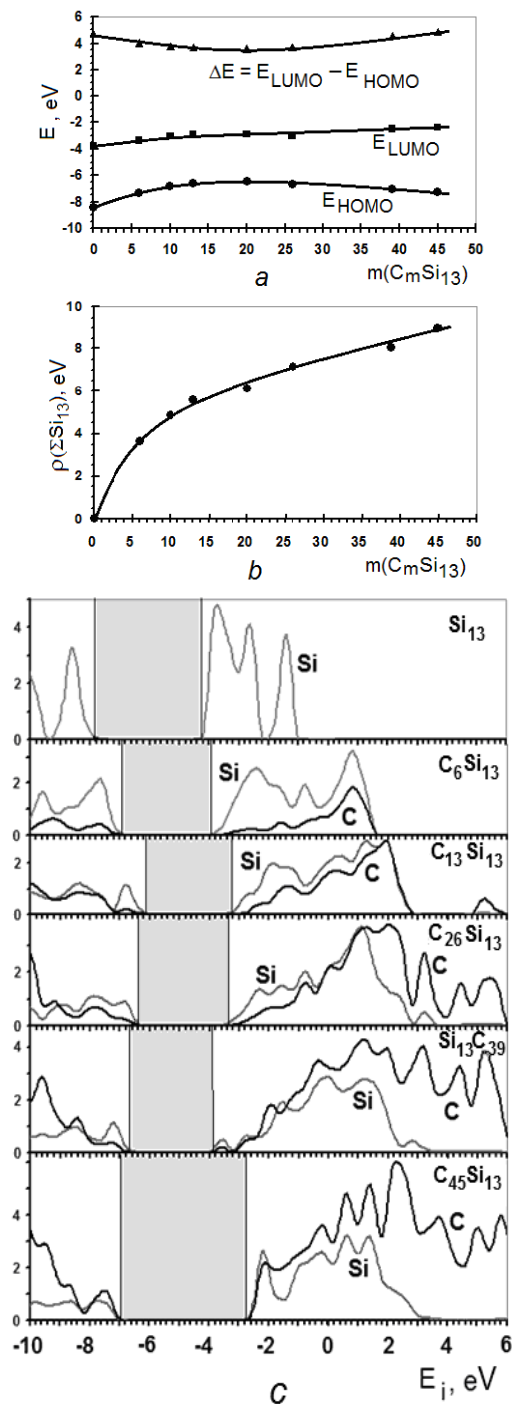

It was noticed in [5] that clusters Si_n had band structure of the density state functions whereas in alloys Li_kSi_n the electron systems of subsystems Si_n and Li_k were united into general one. Analogous picture is also observed for nanoalloys $Li_kC_mSi_n$. An analysis of the frontier molecular orbitals (E_{HOMO} and E_{LUMO}, Fig. 3 *a*) and of local local (over C and Si atoms, Fig. 3 *c*) density state functions testify that both electron donor and electron acceptor properties of C_m subclusters are determined by donor-acceptor characteristics of Si_n subcluster in C_mSi_n nanocomposite are determined by the concentration ratio of silicon and carbon atoms.

In this study, the main attention is paid to the effect of lithiating Si_n nanoclusters and C_mSi_n nanocomposites on their forms and sizes (volume). Initial coordinates of litium atoms in Li_kSi_n and $Li_kC_mSi_n$ nanoalloys under lithiating Si_n and C_mSi_n were also calculated by molecular mechanics method followed by calculation of the electronic structure with semiempirical quantum chemical method PM3. As examples, nanoalloys Li_kSi_{13} and $Li_kC_{10}Si_{13}$ ($k = 0 \div 52$, $k/n = 0 \div 4$) were chosen.

Due to lithiating Si_{13}, a Li_kSi_{13} nanoalloy (Fig. 4) is formed; at the same time, at $k/n \leq 3.08$ in Li_kSi_{13} the volume of nanosystem $V(Li_kSi_{13})$ becomes 2.9 times greater whereas that of silicon matrix (subcluster) $V(Si_{13})$ increases only for 4.25 %. The increase in number of lithium atoms up to 42 ($k/n = 3.23$) and more results in the fracture of initial nanocluster Si_{13} – smaller $Si_{n<13}$ subclusters are formed, each of them having own lithium coat. This testifies penetration of lithium atoms inside nanocluster Si_{13}. The total volume of $Li_{52}Si_{13}$ nanoalloy is 3.5 times greater than that of initial Si_{13} nanocluster; at the same time, the volume of silicon matrix $V(Si_{13})$ in the nanoalloy becomes 1.8 times greater. One can believe that in electrode materials of Li_kSi_n at the lithiation level $k/n > 3.08$ both silicon and lithium atoms are spread in the bulk of nanosystem practically evenly with formation of a lithium-silicon alloy.

Unlike this, when lithiating nanocomposite $C_{10}Si_{13}$ (Fig. 4), its structure iss not changed practically, the volume values of silicon-carbon matrix $V(C_{10}Si_{13})$ increase only for 4.72 %. At $k/13 \leq 1$ lithium atoms do not penetrate into Si/C matrix but take places outside $C_{10}Si_{13}$ subcomposite. Analogous results are true for $C_{13}Si_{13}$ nanocomposite.

Nevertheless, the process of lithiating C_mSi_n nanocomposites at ratio $m/13>1$ ($n=13$, $m=26$, 39, 45; $k=4 \div 52$) with concentration of carbon atoms of 37.2, 46.1, and 59.7 % respectively occurs

Fig. 3. Effect of the number of carbon atoms on the energy values of frontier molecular orbitals E_{HOMO} and E_{LUMO} (*a*), on the total charge of silicon atoms (*b*) and local state functions over atoms Si and C (*c*) in C_mSi_{13} nanocomposites

differently. This is caused by destruction of the initial structure of Si_n subcluster and by formation of carbon associates $C_{m \le n}$ (see Fig. 2) in these nanosystems, so the structure of silicon-carbon matrix at $m/n>2$ becomes more friable. In carbon C_m subcluster pores can be formed where lithium atoms are accumulated under lithiation, so that the limiting ratio of numbers of lithium and silicon atoms k/n (penetration degree of lithium atoms into silicon matrix) in such alloys can be greater than the optimum value (3.75) found experimentally.

It was shown in [5] that the process of lithiating Si_{12} clusters resulted in their essential deformation caused by three time increase in the $V(Li_{k=0-48}Si_{12})$. Analogous regularities were also observed for silicon-carbon composites simulated by $Li_{k=0-52}C_{m(0,6,10,18,26)}Si_{13}$ nanoalloys (Fig. 5 *a*, *b*). The volume values of Si/C nanocomposites after lithiation $V(Li_{k=0-52}C_{m(0,6,10,18,26)}Si_{13})$ (see Fig. 5 *a*) increase linearly (correlation coefficients of 0.997–0.999) with increasing concentration of lithium atoms.
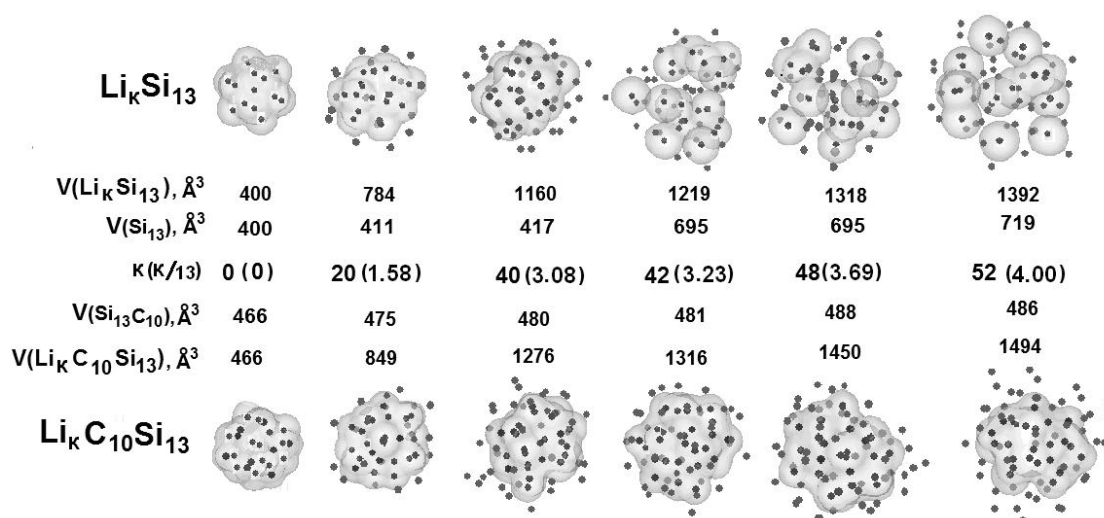

Li_KSi_{13}						
$V(Li_KSi_{13})$, Å³	400	784	1160	1219	1318	1392
$V(Si_{13})$, Å³	400	411	417	695	695	719
к (к/13)	0 (0)	20 (1.58)	40 (3.08)	42 (3.23)	48 (3.69)	52 (4.00)
$V(Si_{13}C_{10})$, Å³	466	475	480	481	488	486
$V(Li_KC_{10}Si_{13})$, Å³	466	849	1276	1316	1450	1494
$Li_KC_{10}Si_{13}$						

Fig. 4. Allocation of Li atoms in nanoalloys when lithiating Si_{13} nanocluster and $C_{10}Si_{13}$ nanocomposite
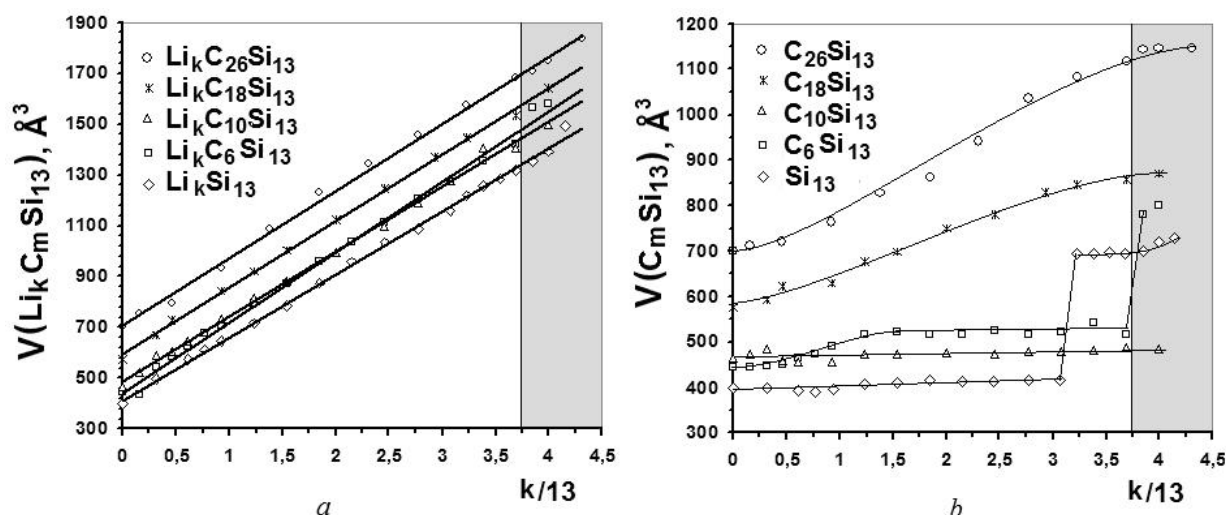

Fig. 5. Effect of the lithiathion process on the volume values of nanoalloys $V(Li_kC_mSi_{13})$ (*a*) and of silicon-carbon subcomposites $V_k(C_mSi_{13})$ $Li_kC_mSi_{13}$ in nanoalloys (k→ 0–52, m→0, 6, 10, 18, 26) (*b*)

Quite another character of such dependences is observed for the electroactive part of Si/C-electrode materials – $C_{m(0,6,10,18,26)}Si_{13}$ subcomposites (Fig. 5 *b*). When lithiating Si_{13} cluster within $0 \leq k/13 \leq 3.08$, the volume of silicon matrix $V_\kappa(Si_{13})$ does not change practically – its average value is 409 Å^3 (± 2 %). The increase in ratio $k/13$ from 3.08 to 3.23 results in hopping increase in the matrix volume up to 697$\pm$8 Å^3 (for 43 %), that value does not change practically due to following increase in the value $k/13$. Such an increase in $V_{\kappa/13=3,23}(Si_{13})$ (see Fig. 4) due to lithiating Si_{13} silicon cluster is caused by formation of more small $Li_{k'<k}Si_{n'<13}$ clusters and, according to [11], can be determined by a change in the structural states of silicon component of the nanoalloy.

From the point of view of the creation of promising Si/C electrodes, in this work such systems were simulated by $C_{m(6,10,18,26)}Si_{13}$ nanocomposites, their volume stability of silicon-carbon matrix $V_{\kappa/13}(C_mSi_{13})$ under lithium atoms penetration is determined by the percentage of carbon atoms in the composite (see Fig. 5 *b*). When lithiating the C_6Si_{13} nanocomposite (16.5 % C), the volume firstly increases droningly from 445 to 515 Å^3 (for ~16 %) at $k/13 \rightarrow 0 \div 1.231$ and is kept stable up to $k/13=3.692$ within ± 1.5 %. At $k/13=3.846$ a hopping increase takes place in the system volume to 781 Å^3 (for ~52 %) that value being kept stable practically under further increase in the concentration of lithium atoms.

Lithating $C_{10}Si_{13}$ composite (24.8 % C) within $k/13=0 \div 4$ does not change the volume of silicon-carbon subcomposite that value being equal to 473 Å^3 within ± 1.9 %. When lithiating composites with greater carbon content – $C_{18}Si_{13}$ (37.2 % C) and $C_{26}Si_{13}$ (46.1 % C), the volume values of silicon-carbon subcomposites change droningly (Fig. 5 *b*) from 575 to 871 Å^3 (inceases for 51.5 %) and from 870 to 1146 Å^3 (increases for 63.5 %) respectively. The results obtained can mean that for Si/C electrode materials these is a clear limit of carbon percentage (~25–30 %) when the process of lithiating material does not effect practically on its geometric parameters (dimensions of C_mSi_n nanocomposites). This fact coincides with the experimental data [11] for Si/C electrodes (sample 1) with the best field-performance and electrochemical data. According to our calculations, the Si/C systems with carbon content less than 17 % ($C_{m \leq 6}Si_{13}$ nanocomposites, samples 2, 4 [11]) or more than 35 % ($C_{m \geq 18}Si_{13}$

nanocomposites, samples 5, 6 [11]) cannot meet the requirements of necessary mechanica stability as due to lithiation at $k/13 \rightarrow 0 \div 4$ great volume expansion (>50 %) of silicon-carbon matrix takes place in such systems. Nevertheless, it is necessary to note that in the Si/C systems the limiting value of carbon content may also depend on the size, structure, atomic coordination type in Si_n and C_m clusters as well as on the lithium diffusion coefficients for silicon and carbon matrices [11].

One of the important merits of any accumulator is the number of charge/discharge cycles without noticeable worsening of the electrochemical characteristics of electrodes (here those of nanocomposite Si/C electrodes). It is also important for the charge/discharge process not to change the spatial structure (volumes) of the electroactive composite Si/C electrodes (C_mSi_n nanocomposites). We have analysed this effect of carbon percenrage in the $C_{10}Si_{13}$ nanocomposites (24.8 % C) and $C_{26}Si_{13}$ (43.1 % C) for two charge/discharge cycles (lithiation – $k/13 \rightarrow 0 - 4$ and delithiation – $k/13 \rightarrow 4 - 0$). It is seen from Fig. 6 that the first $C_{10}Si_{13}$ lithiating cycle results in:

− 3.2 times increase in volume of $Li_{52}C_{10}Si_{13}$ alloy as compared to the initial one of the composite whereas the volume of silicon-carbon mtrix $V_\kappa(C_{10}Si_{13})$ increases only for 4.5 %;

− increase in electron donor capability and decrease in electron acceptor one (a positive shift of E_{OHOMO} for 1.26 eV and that of E_{LUMO} for 1.07 eV) as compared to those of the initial $C_{10}Si_{13}$ composite;

− negligible (for 0.43 eV) decrease in the width of forbidden zone $\Delta E=E_{HOMO}-E_{LUMO}$.

Delithiation of $Li_{52}C_{10}Si_{13}$ alloy results in practically total recovery of all the characteristics of $C_{10}Si_{13}$ nanocomposite mentioned above. Analogous changes are observed in the second cycle.

It should be noticed that the average volume of silicon-carbon matrix $V_k(C_{10}Si_{13})$ in the $C_{10}Si_{13}$ composite at the initial two charge/discharge cycles is kept stable within ± 2.4 % in both charged and discharged (lithiated) states. The total bonding energies E_{bd} for both initial and delitiated $C_{10}Si_{13}$ composites after two cycles slightly change – the average value $E_{bond}(C_{10}Si_{13}) = -(1038.5 \pm 1.0)$ eV. Analogous regularities are true for the C_6Si_{13} and $C_{13}Si_{13}$ silicon-carbon composites.

Unlike $Li_{52}C_{10}Si_{13}$ alloy, lithiated $Li_{52}C_{26}Si_{13}$ composite after the first and the second cycles demonstrates 2.5 times and 2.3 times increases in volume respectively whereas that of parental

_____

silicon-carbon matrix $V_k(C_{26}Si_{13})$ shows 1.56 times and 1.66 time increase respectively (Fig. 7). The volumes of both initial and delithiated $C_{26}Si_{13}$ composites after the first and the second cycles do not change practically and their average volume is equal to 713 ± 8 Å^3 but cycling these systems results in the essential change in the spatial structure of $C_{26}Si_{13}$ silicon-carbon matrix (Fig. 7) – it becoms more friable, pores and $C_{m(2,3,4)}$ carbon subclusters are formed whereas the Si_{13} subcluster is loosen and destroyed. Analogous regularities are also true for the $C_{39}Si_{13}$ and $C_{45}Si_{13}$ composites.
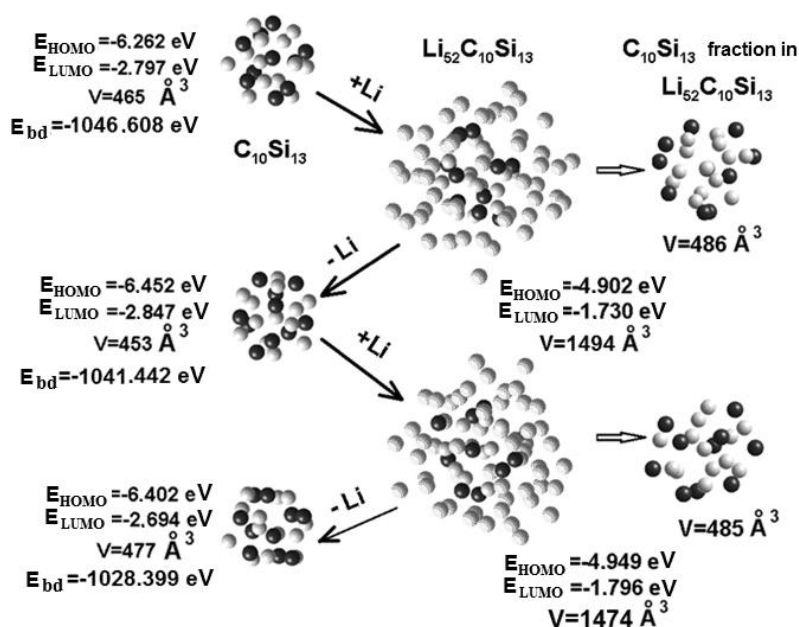

Fig. 6. Changes in electron (E_{HOMO}, E_{LUMO}, and E_{bd}) and structural (V) characteristics of the $C_{10}Si_{13}$ composite in the initial two cycle charge/discharge cycles ($Li_{kk=0-52}C_{10}Si_{13}/Li_{k=52-0}C_{10}Si_{13}$ systems)
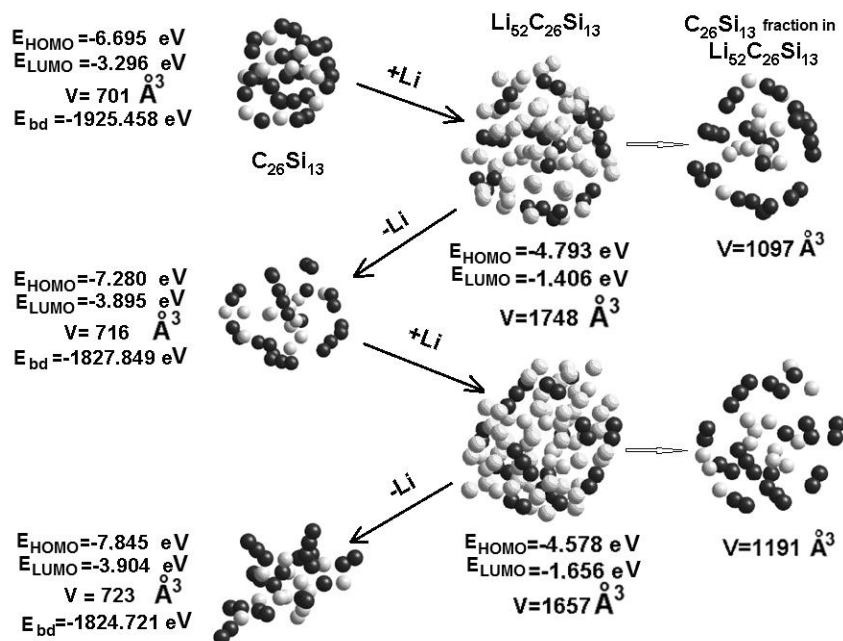

Fig. 7. Changes in electron (E_{HOMO}, E_{LUMO}, E_{bond}) and structural (V) characteristics of $Li_{k=0-52}C_{26}Si_{13})/Li_{k=52-0}C_{26}Si_{13}$ alloys in initial two charge/discharge cycles

Lithiating $C_{26}Si_{13} \rightarrow Li_{к(0 \rightarrow 52)}C_{26}Si_{13}$ composite (Fig. 7) with twice as many carbon atoms as silicon ones results, like in case of $C_{10}Si_{13} \rightarrow Li_{к(0 \rightarrow 52)}C_{10}Si_{13}$ (Fig. 6), in an increase in electron donor capability and in a decrease in electron acceptor one of the $Li_{52}C_{26}Si_{13}$ alloy (a shift of the values E_{HOMO} and E_{LUMO} to more positive energies in both the first and the second cycles).

CONCLUSIONS

For Si/C electrodes where the concentration of carbon atoms does not exceed 25–30 % (model $C_{m=10,13}Si_n$ nanocomposites), the structural characteristics of electrode materials under charge/discharge are more stable essentially than those of relative silicon-based ones (model Si_n clusters) or of materials with content of carbon atoms between 17 and 35 % (model $C_{6 \leq m \leq 18}Si_{13}$ composites). When cycled, such Si/C electrodes are capable to accumulate reversibly large lithium quantities and due to the stable volumes of silicon/carbon matrices should not undergo considerable local periodic mechanical stresses. It means that they can have more reliable electrical contacts between the active material and lead as well as more stable electrochemical characteristics.

When cycling Si/C electrodes with carbon content beyond the 17 to 35 % range (model $C_{m \leq 6}Si_{13}$ and $C_{m \geq 18}Si_{13}$ nanocomposites) sufficiently large mechanical stresses take place, the volumes $V(C_mSi_n)$ of electroactive silicon-carbon matrices due to charge/discharge change for more than 50 %. This can result not only in essential deterioration of lithium-ion batteries but also in their total destruction. Moreover, an increase in the carbon content in C_mSi_n nanocomposites leads to the essential decrease in the specific capacity of the batteries with such electrodes.

Порівняльна квантовохімічна оцінка процесів літіювання/делітіювання в нанокластерах Si$_n$ та нанокомпозитах C$_m$Si$_n$

М.Т. Картель, В.С. Куць, А.Г. Гребенюк, Ю.О. Тарасенко

*Інститут хімії поверхні ім. О.О.Чуйка Національної академії наукУкраїни
вул. Генерала Наумова, 17, Київ, 03164, Україна, kutsvs08@rambler.ru*

Проведено порівняльну квантовохімічну (метод РМ3 2012, 14.083 W) оцінку процесів літіювання/делітіювання нанокластерів Si$_n$ та нанокомпозитів C$_m$Si$_n$. Показано, що в нанокомпозитах (25 та ~30 % C, відповідно) процеси літіювання/делітіювання практично не впливають на об'єми та структуру вихідної (C$_m$Si$_n$), літійованої (Li$_{k=0-52}$C$_m$Si$_n$) та делітійованої (Li$_{k=52-0}$C$_m$Si$_n$) кремній-вуглецевої матриці Si/C. Електроди з таких матеріалів не повинні піддаватися руйнівним періодичним деформаціям в заряд/розрядних циклах. Навпаки, при менших концентраціях вуглецю (нанокомпозит C$_6$Si$_{13}$, ~16 % C) літіювання приводить до стрибкоподібного збільшення V(C$_6$Si$_{13}$) в 1.8 рази, а делітіювання − до зміни структури вихідної кремній-вуглецевої матриці Si/C. Для електродів Si/C з концентрацією вуглецю понад 37 % (композити C$_{m>18}$Si$_n$) літіювання викликає монотонне збільшення об'єму в 1.3 (C$_{18}$Si$_{13}$) та 1.5 (C$_{26}$Si$_{13}$) рази, а делітіювання – до істотної зміни вихідної структури кремній-вуглецевої матриці.

Ключові слова: *нанокластери кремнію, кремній-вуглецеві нанокомпозити, літіювання/делітіювання, питомий об'єм, напівемпіричні квантовохімічні розрахунки*

M.T. Kartel, V.S. Kuts, A.G. Grebenyuk, Yu.A. Tarasenko

_____

Сравнительная квантовохимическая оценка процессов литирования/делитирования в нанокластерах Si_n и нанокомпозитах C_mSi_n

Н.Т. Картель, В.С. Куц, А.Г. Гребенюк, Ю.А. Тарасенко

Институт химии поверхности им. А.А.Чуйко Национальной академии наукУкраины
ул. Генерала Наумова, 17, Киев, 03164, Украина, kutsvs08@rambler.ru

Проведена сравнительная квантовохимическая (метод PM3 2012, 14.083 W) оценка процессов литирования/делитирования нанокластеров Si_n и нанокомпозитов C_mSi_n. Показано, что в нанокомпозитах (25 и ~30 % C, соответственно) процессы литирования/делитирования практически не влияют на объемы и структуру начальной (C_mSi_n), литированной ($Li_{k=0-52}C_mSi_n$) и делитированной ($Li_{k=52-0}C_mSi_n$) кремний-угольной матрицы Si/C. Электроды из таких материалов не должны испытывать разрушительных периодических деформаций в заряд/разрядных циклах. Напротив, при меньших концентрациях углерода (нанокомпозит C_6Si_{13}, ~16 % C) литирование приводит к прыжкообразному увеличению $V(C_6Si_{13})$ в 1.8 раза, а делитирование − к изменению структуры начальной кремний-углеродной матрицы Si/C. Для электродов Si/C с большей концентрацией углерода чем 37 % (композиты $C_{m>18}Si_n$) литирование вызывает монотонное увеличение объема в 1.3 ($C_{18}Si_{13}$) и 1.5 ($C_{26}Si_{13}$) раза, а делитирование к существенному изменению начальной структуры кремний-углеродной матрицы.

Ключевые слова: нанокластеры кремния, кремний-углеродные нанокомпозиты, литирование/делитирование,удельный объем, полуэмпирические квантовохимические расчеты

REFERENCES

1. *Obrovac M.N., Christensen L.* Structural changes in silicon anodes during lithium insertion/extraction, Electrochem. & Solid-State Lett., 7 (2004) A93.

2. *Kasavajjula U., Wang Ch., Appleby A.J.* Nano- and bulk-silicon-based insertion anodes for lithium-ion secondary cells, J. Power Sources, 163 (2007) 1003.

3. *Larcher D., Beattie S., Morcrette M. et al.* Recent findings and prospects in the field of pure metals as negative electrodes for Li-ion batteries, J. Materials Chem., 17 (2007) 3759.

4. *Boukamp B.A., Lesh G.C., Huggins R.A.* All-solid lithium electrodes with mixed-conductor matrix, J. Electrochem. Soc., 128 (1981) 725.

5. *Kuksenko S.P., Kuts V.S., Tarasenko Yu.A., Kartel M.T.* Electrochemical investigations and quantum chemical calculations of the system Si_nLi_m, Chem. Phys. Technol. Surface, 2 (2011) 221 (in Russian).

6. *Yang J., Wang B.F., Wang K. et al.* Si/C composites for high capacity lithium storage materials, Electrochemical and Solid-State Letters, 6 (2003) A154.

7. *Dimov N., Kugino S., Yoshio M.* Mixed silicon–graphite composites as anode material for lithium ion batteries: Influence of preparation conditions on the properties of the material, J. Power Sources, 136 (2004) 108.

8. *Ng S.H., Wang J., Wexler D. et al.* Highly reversible lithium storage in spheroidal carbon-coated silicon nanocomposites as anodes for lithium-ion batteries, Angew. Chem. Int. Ed., 45 (2006) 6896.

9. *Hochgatterer N.S., Schweiger M.R., Koller S. et al.* Winter. Silicon-graphite composite electrodes for high-capacity anodes: influence of binder chemistry on cycling stability, Electrochem. Solid State Lett., 11 (2008) A76.

10. *Khomenko V.G., Barsukov V.Z.* Characterization of silicon-and carbon-based composite anodes for lithium-ion batteries, Electrochimica acta, 52 (2007) 2829.

11. *Roginskaya Y.E., Kulova T.L., Skundin A.M. et al.* The structure and properties of a new type of nanostructured composite Si/C electrodes for lithium ion accumulators, Russ. J. Phys. Chem. A., 82 (2008) 1655.

12. *Zavyalov S.A., Kulova T.L. Kupriyanov L.Y. et al.* The structure and charge-storage

capacitance of carbonized films based on silicon-polymer nanocomposites, Russ. J. Phys. Chem. A., 82 (2008) 2165.

13. *Kuksenko S.P., Kovalenko I.O., Tarasenko Yu.A., Kartel N.T.* Forming a stable amorphous phase in the carbon-coated silicon upon deep electrochemical lithiation, Chem. Phys. Technol. Surface, 1 (2010) 57 (in Russian).

14. *Kuksenko S.P., Kovalenko I.O., Tarasenko Yu.A., Kartel N.T.* Nanocomposite silicon-carbon for hybride electrodes of lithium-ion batteries, Problems of Chem. & Chem. Technol., 4 (2011) 299 (in Russian).

15. *Wilson A.M., Reimers J.N., Fuller E.W., Dahn J.R.* Lithium insertion in pyrolyzed siloxane polymers, Solid State Ionics, 74 (1994) 249.

16. *Holzapfel M., Buqa H., Krumeich F. et al.* Chemical vapor deposited silicon/graphite compound material as negative electrode for lithium-ion batteries, Electrochem. & Solid-State Lett., 8 (2005) A516.

17. *Jung Y.S., Lee K.T., Oh S.M.* Si–carbon core–shell composite anode in lithium secondary batteries, Electrochem. Acta, 52 (2007) 7061.

18. *Yoshio M., Wang H., Fukuda K. et al.* Carbon-coated Si as a lithium-ion battery anode material, J. Electrochem. Soc., 149 (2002) A1598.

19. *Kim B.-C., Uono H., Sato T. et al.* Li-ion battery anode properties of Si-carbon nanocomposites fabricated by high energy multiring-type mill, Solid State Ionics, 172 (2004) 33.

20. *Liu Y., Hanai K., Yang J. et al.* Silicon/carbon composites as anode materials for Li-ion batteries, Electrochem. and Solid-State Lett., 7 (2004) A369.

21. *Schmidt M.W., Baldridge K.K., Boatz J.A. et al.* General atomic and molecular electronic structure system, J. Comput. Chem., 14 (1993) 1347.

22. *Maia J.D.C., Urquiza Carvalho G.A., Mangueira Jr. C.P. et al.* GPU linear algebra libraries and GPGPU programming for accelerating MOPAC semiempirical quantum chemistry calculations, J. Chem. Theory & Comput., 8 (2012) 3072.

23. *Iwamatsu M.* Global geometry optimization of silicon clusters using the space-fixed genetic algorithm, J. Chem. Phys., 112 (2000) 10976.

24. *Li B.-X., Cao P.-L., Zhan S.-C.* Ground state structures of Si$_n$ (n = 11–25) clusters, Phys. Lett. A., 316 (2003) 252.

25. *Zhu X.L., Zeng X.C., Lei Y.A., Pan B.* Structures and stability of medium silicon clusters. II. *Ab initio* molecular orbital calculations of Si$_{12}$–Si$_{20}$, J. Phys., 120 (2004) 8985.